LM-06K052
May 11, 2006

Accurate Method for Forward and Reverse Bias Curve Fitting of TPV I-V Data

L Danielson and D Depoy

Accurate Method for Forward and Reverse Bias Curve Fitting of Thermophotovoltaic I-V Data

L.R. Danielson and D.M. Depoy
Lockheed-Martin, Schenectady, N.Y.

Abstract

An automated current-voltage curve fitting method has been developed for thermophotovoltaic (TPV) cells. TPV cells are similar to solar cells except TPV cells utilize the infrared portion of a hot radiator spectrum instead of the solar spectrum. The method is automatic, accurate, fast, and simple. The fit is based on a two diode model with one diode having n_1=1 and the second diode having n_2=2. The program extracts saturation currents for the n_1=1 and n_2=2 terms, series resistance, shunt resistance, light-generated current, breakdown current, and breakdown voltage. Only one curve with forward bias data and optional reverse bias data is necessary as input. Two curves can be inputted if one curve has forward bias data and the other has reverse bias data. The model has successfully fitted both ternary and quaternary cells with a wide range of cell parameters. Differences between the fit and the data are generally smaller than 0.5% for short-circuit current, open-circuit voltage, fill factor, and maximum power. The curve-fitting methodology is also expected to be applicable to solar cells.

Introduction

Thermophotovoltaic (TPV) energy conversion is the direct conversion of infrared radiation into electricity by means of a photodiode (1, 2). The current-voltage (I-V) curves generated by TPV diodes (cells) are very similar to solar cell I-V curves, although TPV cells are often tested under reverse bias as well as forward bias conditions. To the authors' knowledge, there is so far no published literature specifically regarding the curve-fitting of I-V curves generated by TPV cells. The present paper describes a novel curve-fitting method that is expected to be applicable to solar cells as well as TPV cells.

There are several I-V curve fitting methods reported for solar cells. An early paper (3) fits the I-V curve to a single exponential including series and shunt resistances. Other investigators have focused on determining series resistance (4-7), fitting I-V curves to a single exponential model (8-12), or fitting to a two exponential model (13-17).

Many of the models in the literature fit five parameters simultaneously using a least squares approach to minimize the error. The model in this paper (TRIVET) is different in that it determines five cell parameters in a particular well-defined order, and then determines the reverse bias parameters. One advantage of determining parameters sequentially rather than simultaneously is that the effect of shunt resistance can be separated from the effects of idealities and saturation or recombination currents. Also, the initial determination of the saturation and recombination currents is independent of the series resistance. The present approach is simple and highly accurate, and has been used extensively at Lockheed Martin to successfully fit TPV I-V curves.

It has been found experimentally that TPV cells with InGaAsSb epilayers grown lattice matched on GaSb substrates can be well-fit to a single exponential model, whereas TPV cells with

InGaAs epilayers grown lattice mismatched on InP substrates are better fit with a two exponential model. In this paper the topic is limited to a two exponential model plus an additional optional exponential term for the reverse bias condition. This two exponential model can be effectively used for either lattice matched InGaAsSb or lattice mismatched InGaAs cells.

Curve-fitting Method

Fitting of the TPV I-V curves is accomplished using Eq. 1. The n_1=1 term and the n_2=2 terms account for the nonlinearity in the ln(I_{SC}) vs. V_{OC} plots, especially at low current levels.

$$I = -I_L + \frac{V - IR_S}{R_{SH}} + I_S\left[e^{\frac{q}{n_1 kT}(V - IR_S)} - 1\right] + I_R\left[e^{\frac{q}{n_2 kT}(V - IR_S)} - 1\right] - I_B e^{-\frac{(V - IR_S)}{B}} \qquad \text{Eq. 1}$$

Linear term; n_1=1 term; n_2=2 term; reverse bias term

The seven independent parameters to determine in Eq. 1 are the light generated current, I_L, the series resistance R_S, the shunt resistance, R_{SH}, the reverse breakdown current, I_S, the recombination current I_R, the breakdown current, I_B, and the breakdown parameter B. I_L is a positive number and I_{SC} is a negative number.

Empirical modeling of the reverse bias current of the TPV I-V curve with a temperature-independent exponential dependence results in a good fit for V<0 for single junction quaternary and ternary cells as well as multi-junction Monolithically Interconnected Modules (MIMs). Other photodiodes, e.g., silicon solar cells, with different doping levels and different reverse bias breakdown mechanisms may not be well fitted by an exponential in the reverse bias region.

Several inputs are necessary to generate the desired output parameters. The single forward bias input curve is acquired under illuminated conditions. Either an illuminated or a dark I-V curve with reverse bias data can be input for optional determination of reverse bias parameters. Other inputs are the number of junctions in series, and the voltage region where the shunt resistance should be determined. The initial estimate of the series resistance is zero. The outputs are the seven parameters in Eq. 1 together with the open-circuit voltage (V_{OC}), the short-circuit current (I_{SC}), the maximum power (P_{max}), the voltage and current at maximum power, and the fill factor [FF = $P_{max}/(I_{SC}V_{OC})$]. The order of determining the parameters is important and is outlined in Figure 1 and below.

Step 1 – Determination of the Shunt Resistance, R_{SH}

The shunt resistance of the cell is determined by taking the derivative of the I-V curve (Eq. 1) and solving for R_{SH}. The result is

$$R_{SH} = \frac{1 - R_S S}{S - (1 - R_S S)\left[\frac{qI_S e^{\frac{q(V - IR_S)}{kT}}}{kT} + \frac{qI_R e^{\frac{q(V - IR_S)}{2kT}}}{2kT} + \frac{I_B e^{-\frac{(V - IR_S)}{B}}}{B}\right]} \qquad \text{Eq.2}$$

$$R_{SH} = \frac{1 - R_S S}{S - (1 - R_S S)[\text{Term1} + \text{Term2} + \text{Term3}]}$$

where S≡dI/dV.

The three terms inside the square brackets in Eq. 2 and the sum of these terms are plotted as a function of voltage for a single-junction ternary cell (Fig. 2) and for a ternary Monolithically Interconnected Module (MIM) (Fig. 3). These three terms are negligible compared to the slope, S, except at very high shunt resistances. Since the I-V curve for a cell or MIM is not appreciably changed for shunt resistances above approximately 30 ohms, this uncertainty in calculating high shunt resistances is not detrimental. A good approximation to the shunt resistance with negligible contribution from the three terms in Eq. 2 is then

$$R_{SH} = \frac{1}{S} - R_S \qquad \text{Eq. 3}$$

The expression in Eq. 3 is used in the curve fitting program. Physically, the intrinsic diode property of shunt resistance does not depend on the diode series resistance. However, increasing either the series resistance or shunt resistance of a diode will lower the slope of the I-V curve, so the effect of series resistance must be subtracted out in order to accurately calculate shunt resistance.

There is an optimum region for calculating the slope, S, as shown in Figures 2 and 3. This region of negative voltage should be far enough from zero so that the forward bias terms are minimal, and in addition, close enough to zero so that the reverse bias term is also minimal. In practice, this region seems to be -0.1 and -0.6 volts, although this can vary. For example, if the reverse breakdown voltage is several volts, the slope of the I-V curve could be computed at larger negative values than -0.6 volts. The first time R_{SH} is calculated, the series resistance in Eq. 3 is set equal to zero. For Steps 5 and 6, the shunt resistance is recalculated based on the series resistance calculated in Step 4.

Step 2 – Determination of the Light-Generated Current, I_L

The second step in fitting I-V data to Equation 1 is to find an expression for the light-generated current, I_L. I_L is a constant for all voltages, and it is most convenient to determine I_L at V = 0, I = I_{SC}. In this case solving Eq. 1 for I_L and neglecting the negligible exponential terms at V = 0 yields

$$I_L = -I_{SC}\left(1 + \frac{R_S}{R_{SH}}\right) \qquad \text{Eq. 4}$$

In Step 2, the initial series resistance in Eq. 4 is zero, and the shunt resistance is the shunt resistance calculated in Step 1. For Steps 5 and 6, I_L is recalculated based on the series resistance calculated in Step 4 and the shunt resistance calculated in Step 1.

Step 3 – Determination of the I_S and I_R currents

The saturation current (I_S) and the recombination current in the depletion region (I_R) are calculated in Step 3. The maximum negative value for the reverse bias term for voltages greater than zero is $-I_B\exp(IR_S/B)$. This maximum value equals approximately $-6\text{x}10^{-5}$A for a ternary single junction cell and $-5.8\text{x}10^{-5}$A for a ternary MIM. Thus, it is generally acceptable to ignore (except for extremely small I_{SC} values) the contribution of the reverse bias term to the forward bias calculations.

Two points, (I_1,V_1) and (I_2,V_2) are selected on the I-V curve. The selection of the two points on the I-V curve is chosen so the ideal parameters are calculated in a region of interest near the maximum power point. Good results are achieved with I_1 and V_1 as the current and voltage at the maximum power point, and I_2 and V_2 are the current and voltage at the open-circuit voltage point (I_2 =0). I_S and I_R are found from solving Eq. 1 with two equations with two unknowns and neglecting the reverse bias term. The results are

$$I_S = \frac{b\left(I_2 + I_L - \frac{y_2}{R_{SH}}\right) - d\left(I_1 + I_L - \frac{y_1}{R_{SH}}\right)}{bc - ad}, \qquad \text{Eq.5}$$

and

$$I_R = \frac{I_2 + I_L - \frac{y_2}{R_{SH}} - cI_S}{d} \qquad \text{Eq.6}$$

where

$y_1 = V_1 - I_1R_S$, $y_2 = V_2 - I_2R_S$, $a = e^{zy_1} - 1, b = e^{\frac{zy_1}{2}} - 1, c = e^{zy_2} - 1, d = e^{\frac{zy_2}{2}} - 1$, and $z = \frac{q}{kT}$.

Step 4 – Determination of the Series Resistance, R_S

The actual series resistance is calculated by selecting a forward bias (positive) current, I_p, which is fixed at 90% of the maximum forward bias current, and determining the difference between the experimental data and the fitted curve up through Step 3 with $R_S = 0$. The series resistance is then

$$R_S = \frac{V_4 - V_3}{I_p}, \qquad \text{Eq. 7}$$

$$B = \frac{x_5 - x_6}{\ln\left(\frac{-I_L - I_6 + \frac{x_6}{R_{SH}}}{-I_L - I_5 + \frac{x_5}{R_{SH}}}\right)}, \qquad \text{Eq . 9}$$

calculated from
where V_4 = the voltage at I_p for the data, and V_3 = the voltage at I_p for the fit.

Step 5 -- Comparison of the Fit to the Previous Iteration

The fit parameter is determined by the sum of the squares of the differences between the fit and the data for the open-circuit voltage (V_{OC}), the short-circuit current (I_{SC}), the fill factor (FF), and the maximum power (P_{max}). That is,

$$\text{Fit Parameter} = \left[\Delta V_{OC}^{\ 2} + \Delta I_{SC}^{\ 2} + \Delta FF^{\ 2} + \Delta P_{max}^{\ 2}\right]^{0.5} \qquad \text{Eq. 8}$$

where the delta's represent the difference between the fit and the data at P_{max}.

Step 6 -- Determination if this is the last iteration

If the fit parameter is greater than the previous iteration, the fitting procedure continues with Step 7 with the previous iteration values. If the fit accuracy is less than the previous iteration, the fitting procedure returns to Step 1.

Step 7 -- Determination of the Reverse Bias Parameters, I_B and B

The reverse breakdown parameters are calculated in Step 7. The maximum value for the n_1=1 term in the reverse bias region is $-I_S$, and the maximum value for the n_2=2 term in the reverse bias region is $-I_R$. Since these terms are generally small ($<10^{-3}I_{SC}$) relative to the reverse bias term for both single and multi-junction cells, the reverse bias term is determined independently of the forward bias n_1=1 and n_2=2 terms.

The curve-fitting program has the option to use either a light or a dark I-V curve for determination of the reverse bias parameters. The I-V curve to be used can either be the same as the illuminated curve, or it can be a different I-V curve (dark or illuminated). If an illuminated curve is used for the reverse bias parameter determination, the light generated current is subtracted out. The fit is accomplished by selecting two points (V_5, I_5 and V_6, I_6) on the reverse breakdown portion of the curve. The best fits have been found empirically to be when $V_5 = 0.76V_{max}$ and $V_6 = 0.84V_{max}$, where V_{max} is the maximum negative voltage on the I-V curve. Equation 1 without the forward bias terms is solved with two equations and two unknowns. The expression for B is

And for I_B is

$$I_B = e^{\frac{x_6}{B}}\left[-I_L - I_6 + \frac{x_6}{R_{SH}}\right] \qquad \text{Eq . 10}$$

where

$$x_5 = V_5 - I_5 R_S, \text{ and } x_6 = V_6 - I_6 R_S.$$

Step 8 -- Final Calculation

The experimental I-V curve is fit with a single equation including all terms in forward and reverse bias. The fitted values of V_{OC}, I_{SC}, FF, and P_{max} are determined and compared to the data.

Results

An initial check was performed to determine the ability of a program to correctly fit a simulated I-V curve based on typical TPV cell parameters. The excellent fit is shown in Figure 4 and Table 1.

Parameter	**Input Parameters**	**I-V Values from Input Parameters**	**Fit Parameters**	**% Difference**
Isc (A)	0.256	0.256	0.256	$<1.0 \times 10^{-11}$
Voc (V)		0.394	0.394	$<1.0 \times 10^{-11}$
FF (%)		72.1	72.1	$<1.0 \times 10^{-11}$
P_{max} (W)		.0726	.0726	$<1.0 \times 10^{-11}$
I_S (A)	4.92×10^{-8}		4.94×10^{-8}	0.41
I_R(A)	1.59×10^{-5}		1.52×10^{-5}	4.4
R_S (Ω)	0.0400		.0404	1.0
R_{SH} (Ω)	129		117	9.3
I_B (A)	5.7×10^{-5}		5.25×10^{-5}	7.9
B (V)	0.270		0.269	0.37

Table 1. Comparison of simulated data based on typical TPV cell values and the fit.

The curve fitting has been found to be accurate for single junction cells with areas of 0.5cm^2 as well as multi-junction MIMs with areas of 1-4cm^2. For the MIMs, typically with 25-30 junctions, the input voltage is divided by the number of junctions to obtain equivalent single junction properties for the MIMs. This assumes that all individual single junction areas can be fitted by the same parameters, and this is generally observed in practice.

The fit accuracies for a group of 88 MIMs are shown in Table 2, where the percent difference is between the actual and the curve-fitted data. The table shows the excellent fits for all the MIMs, with an average difference for the maximum power of about 0.3%. The average number of iterations was about 5, and the total time for a curve fit was about 5 seconds.

Parameter	**Average % Difference**
Isc (A)	0.0056

Voc (V)	0.103
FF (%)	0.32
P_{max} (W)	0.28

Table 2. Absolute values of the percent differences between each fit and the data for each of 88 MIMs.

A parameter that can be easily calculated from the fit is an f-factor, which is the ratio of the n_2=2 term to the n_1 =1 term in Eq. 1. That is, the f-factor represents the relative contribution of the depletion regions and active regions to the overall current. The expression for the f-factor, f, is given in Eq. 11.

$$f = \frac{I_R\left[e^{\frac{q}{2kT}(V-IR_S)} - 1\right]}{I_S\left[e^{\frac{q}{kT}(V-IR_S)} - 1\right]} \qquad \text{Eq.11}$$

A plot of the fill factor as a function of the f-factor (Fig. 5) shows that increasing the contribution of the n_2=2 term decreases the fill factor. Thus, the f factor should be reduced as much as possible to maximize the fill factor and the conversion efficiency. For comparison, the f-factor for lattice-matched InGaAsSb on GaSb is approximately 0.1 – 0.2.

The parameters extracted by the method described above were used to predict the performance of three MIMs at different temperatures and light generated currents. In particular, the parameters were extracted for short-circuit currents of approximately 0.2A – 0.45A, and for a MIM temperature of 25C. The following analysis compares the predicted and measured electric power for currents up to 0.55A and temperatures up to 80C . The MIM characteristics at 25C for the three cells are given in Table 3. The MIMs had slightly different architectures and varied in area from 4cm^2 to 5.2 cm^2, and contained from 25 to 30 n-p junctions.

MIM	Cell Parameters at 25C			
	Series Resistance (Ω)	Shunt Resistance (Ω)	I_S (A)	I_R (A)
Sample A	0.082	403	1.73×10^{-8}	3.73×10^{-5}
Sample B	0.018	29	2.68×10^{-8}	1.81×10^{-4}
Sample C	0.041	120	7.33×10^{-8}	1.04×10^{-4}

Table 3. Parameters for three MIMs measured at 25C.

Measured and predicted electrical powers as a function of light generated current for the three MIMs in Table 3 are presented in Figure 6. Predicted values of power are easily obtained by changing I_L in Eq. 1. Agreement between measured and predicted powers is very good and is within 4% for light-generated currents between 0.15A and 0.58A.

The predicted electrical power as a function of MIM temperature was obtained by calculating the

temperature dependence of I_S and I_R as well as inserting the correct temperature into the exponentials in Eq. 1. Assuming I_S is proportional to the square of the intrinsic carrier concentration, n_i,

$$I_{S1} = I_{S0} \frac{T_1^3 e^{-\frac{E_{G1}}{kT_1}}}{T_0^3 e^{-\frac{E_{G0}}{kT_0}}}, \qquad \text{Eq. 12}$$

where the "0" subscript refers to the initial measured MIM temperature of 25C and the "1" subscript refers to the new temperature, and E_G is the temperature-dependent bandgap. Assuming I_R is proportional to the intrinsic carrier concentration,

$$I_{R1} = I_{R0} \left[\frac{T_1^3 e^{-\frac{E_{G1}}{kT_1}}}{T_0^3 e^{-\frac{E_{G0}}{kT_0}}} \right]^{0.5}, \qquad \text{Eq. 13}$$

In both Eq. 12 and Eq. 13, the dependence of bandgap on temperature is calculated from the following expression for nominal 0.6 eV material:

$$E_G = 0.6955 - (0.00031)T, \qquad \text{Eq. 14}$$

where T is in degrees Kelvin and E_G is in electron volts.
Using Eqs. 12-14 in Eq. 1, the electrical power is calculated for temperatures of 25C - 80C (Figure 7). Excellent agreement (within 1%) is obtained showing the validity of the assumptions.

Discussion

Single diode model

A "basic" multi-illumination approach for finding diode parameters for a single diode model is to measure the cell under several illumination levels, and then find the ideality and the saturation current from the slope and intercept of a $\ln(I_{SC})$ vs. V_{OC} plot. The series resistance is then obtained from the behavior of the I-V curve at high current levels. This manual "basic" approach is relatively labor-intensive, time consuming, and subject to uncertainty regarding the definition of "high current level".

Two diode model

The "basic" multi-illumination approach can also be used for finding diode parameters for a two diode model. The $\ln(I_{SC})$ vs. V_{OC} plot is separated into two linear regions, and two idealities and two saturation currents are computed. The series resistance is then obtained from the behavior of the I-V

curve at high current levels. The voltage at which to divide the curve into two linear regions as well as the region of the curve to calculate the series resistance are difficult to determine in practice. Since the results are dependent on these voltages, the calculation of the diode parameters is somewhat uncertain.

The present curve-fitting program was developed based on a two diode model with the first diode term having an ideality of unity and the second diode term having an ideality of two (Eq. 1). An advantage of this approach is relative simplicity and excellent accuracy. The quality of the fit is estimated by examining the percent difference between the fit and the data for short-circuit current, open-circuit voltage, fill factor and maximum power. Typical percent differences between the fit and the data are less than 0.5%.

A second advantage of the current curve-fitting method over some curve-fitting methods is that only one I-V curve is required to determine the forward bias parameters instead of two. This single I-V curve can either be measured under dark or light illumination conditions. The reason for needing only one I-V curve is that calculation of ideality generally requires two light levels, while if idealities are fixed at $n_1 = 1$ and $n_2 = 2$, only one curve is required.

A third advantage of the present approach is its simplicity. No initial guesses are necessary, and there are no assumptions about correlations between parameters in different regions of the I-V curve. The entire I-V curve is fit sequentially. The program takes the manual method of plotting $\ln(I_{SC})$ vs. V_{OC} and applies it to two points. The use of relatively few points on the curve to obtain the fit was initially a concern to the authors, but results showed that this was not an impediment to obtaining very accurate fits.

A difference between the present method and most methods is the use of a "Fit Parameter" rather than a least squares difference. The fit parameter technique was adopted because it was considered most important to have an accurate fit near the maximum power point in the fourth quadrant rather than in the first or third quadrants. In practice, the fit was found to be excellent in all quadrants of the I-V curve.

Conclusions

The curve-fitting method has been successfully used for a variety of TPV cells with different characteristics. It has been found to accurately extract parameters for use in modeling of TPV cells at various light levels and temperatures different than used in the curve fitting procedure.

References

1. G.W. Charache, P.F. Baldasarao, L.R. Danielson, et al., J. Appl. Phys., 85 (1999), p2247.
2. E.J. Brown, P.F. Baldasaro, S.R. Burger et al., Proc. IECEC 2004, Providence, RI, Aug. 16-19, 2004.
3. M.B. Prince, J. Appl. Physics 26 (1955), 534-540.
4. R.J. Handy, Solid-State Elect., 10 (1967), 765-775.
5. M. Wolf and H. Rauschenbach, Advanced Energy Conv., 3 (1963), 455-479.
6. G.L. Araujo and E. Sanchez, IEEE Transactions on Electron Devices, ED-29 (1982), 1511-13.

7. K. Rajkanan and J. Shewchun, Solid-State Elect., 22(1979), 193-7.
8. D.S.H. Chan, J.R. Phillips, and J.C.H. Phang, Solid-State Elect., 29(1986) 329-337.
9. S.K. Datta, K. Mukhopadhyay, S. Bandopadhyay, and H Saha, Solid-State Elect., 35(1992), 1667-1673.
10. J.A. Ellis and P.A. Barnes, Appl. Phys. Lett., 76(2000), 124-5.
11. H.J. Queisser, Solid-State Elect., 5(1962), 1-10.
12. M. Chegaar, Z. Ouennoughi, and A. Hoffman, Solid-State Elect. 45(2001), 293-6.
13. G.L. Araujo, E. Sanchez, and M. Marti, Solar Cells, 5(1982), 199-204.
14. A. Hovinen, Physica Scripta T, T54(1994), 175-6.
15. A.R. Burgers, J.A. Eikelboom, A. Schonecker, and W.C. Sinke, Proc. 25th IEEE Photovoltaic Specialists Conference, Washington, D.C., 1996, 569-572.
16. J. Cartensen, G. Popkirov, J. Bahr, and H. Foll, Solar Energy Mat. and Solar Cells, 76(2003), 599-601.
17. M. Haouari-Merbah, M. Belhamel, I. Tobias, and J.M. Ruiz, Solar Energy Mat. and Solar Cells, 87(2005), 225-233.

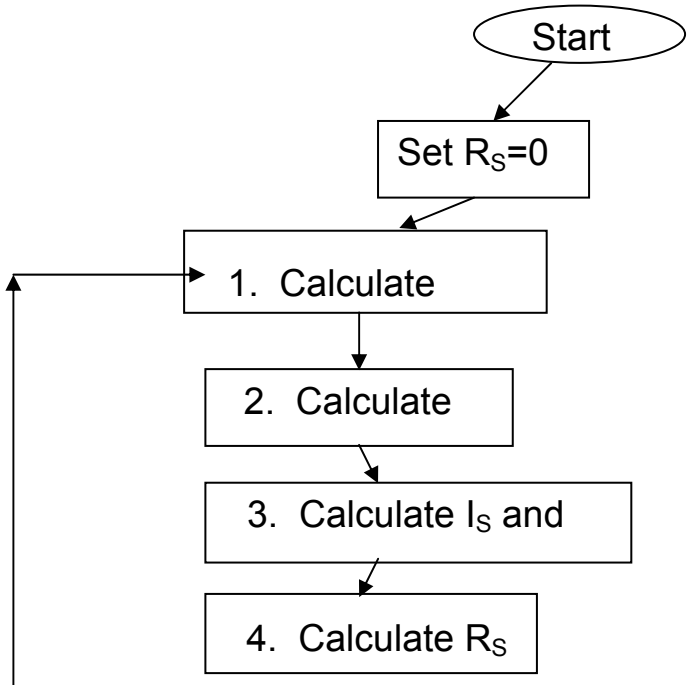

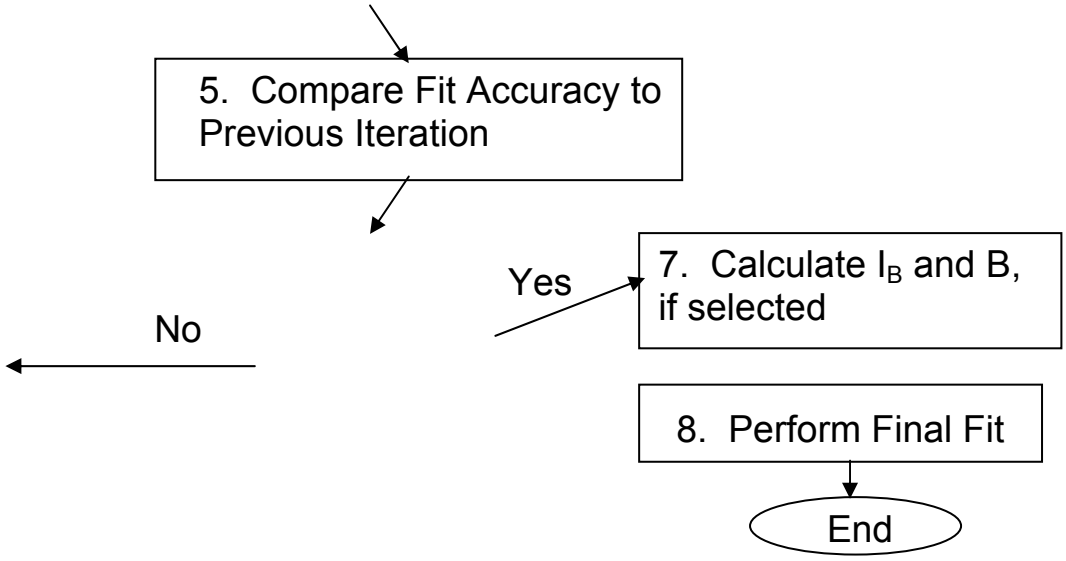

Figure 1. Outline of the sequence of steps performed in the fitting routine.

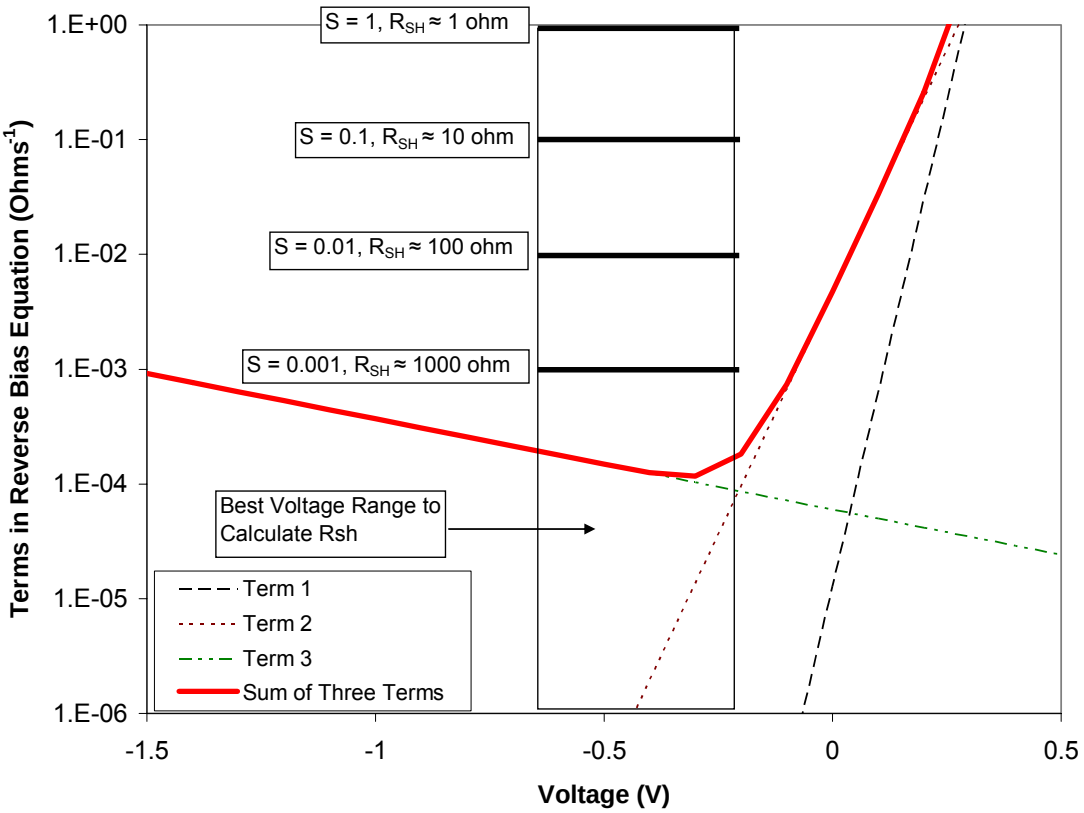

Figure 2. Plot showing the three terms identified in Eq. 2 for a single junction ternary are in general negligible compared to the slope, S, except at very high shunt resistances. The current was taken as the short-circuit current.

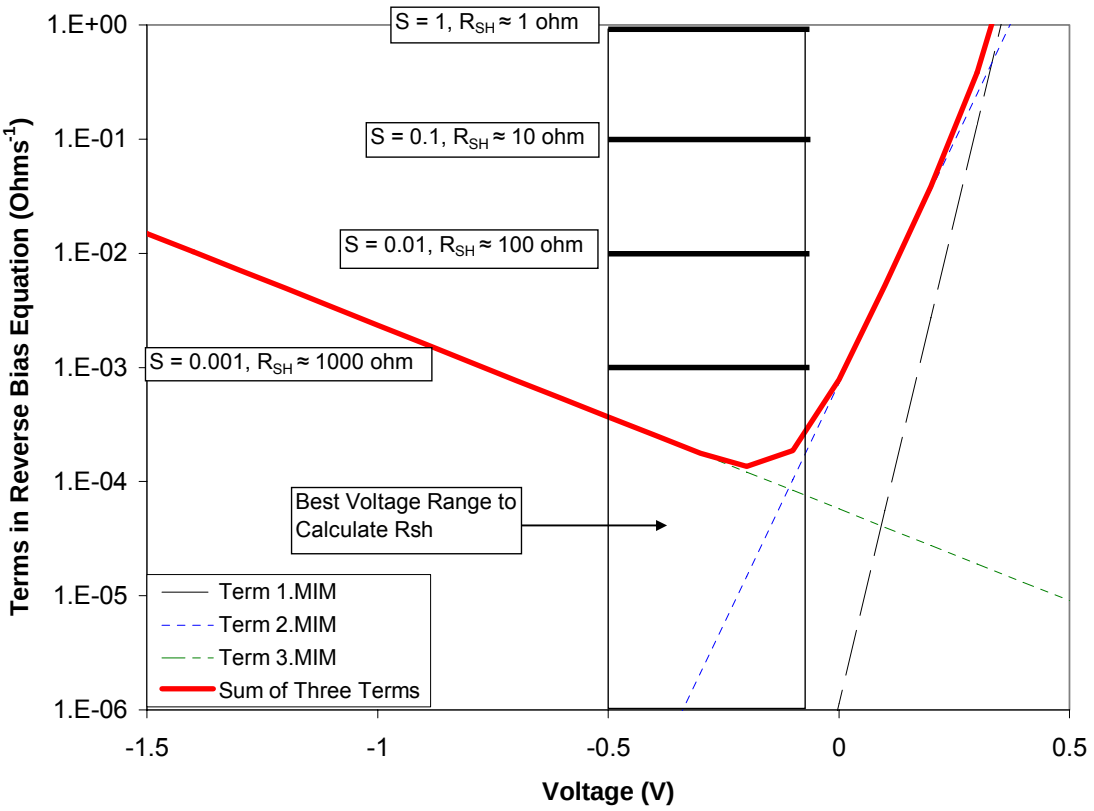

Figure 3. Plot showing the three terms identified in Eq. 2 for a ternary MIM are in general negligible compared to the slope, S, except at very high shunt resistances. The current was taken as the short-circuit current.

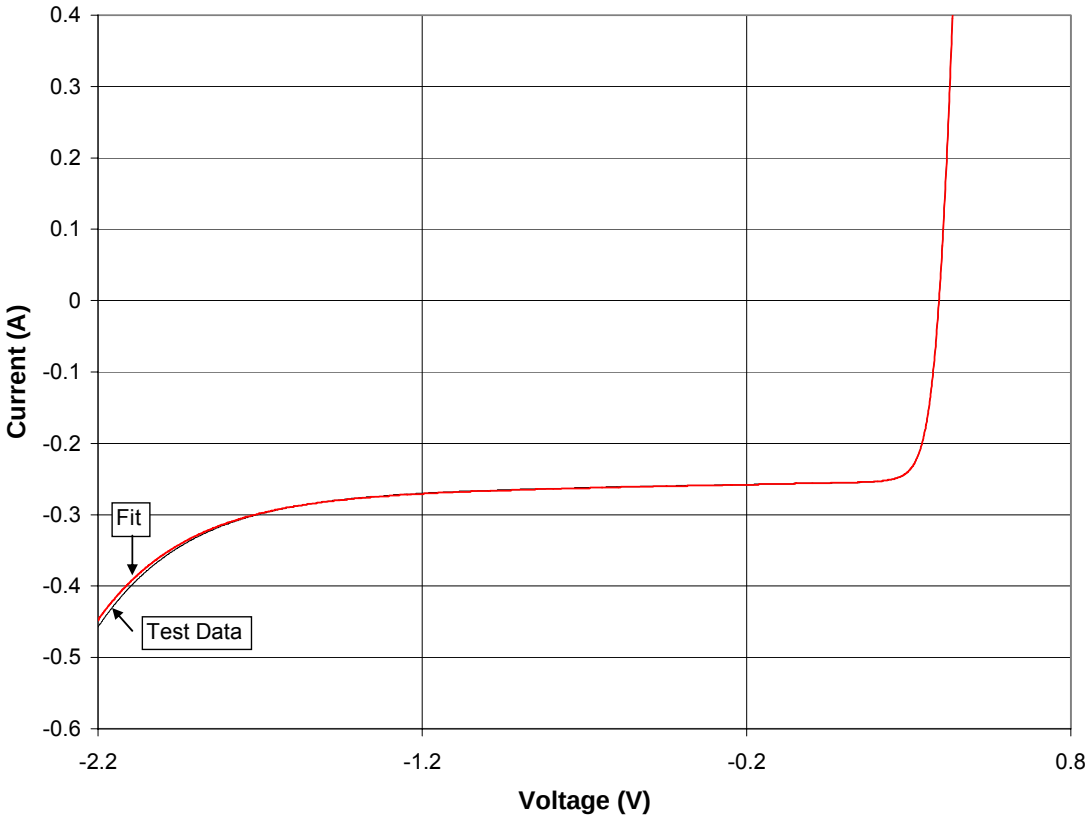

Figure 4. Graph showing excellent agreement between simulated typical test data and fit.

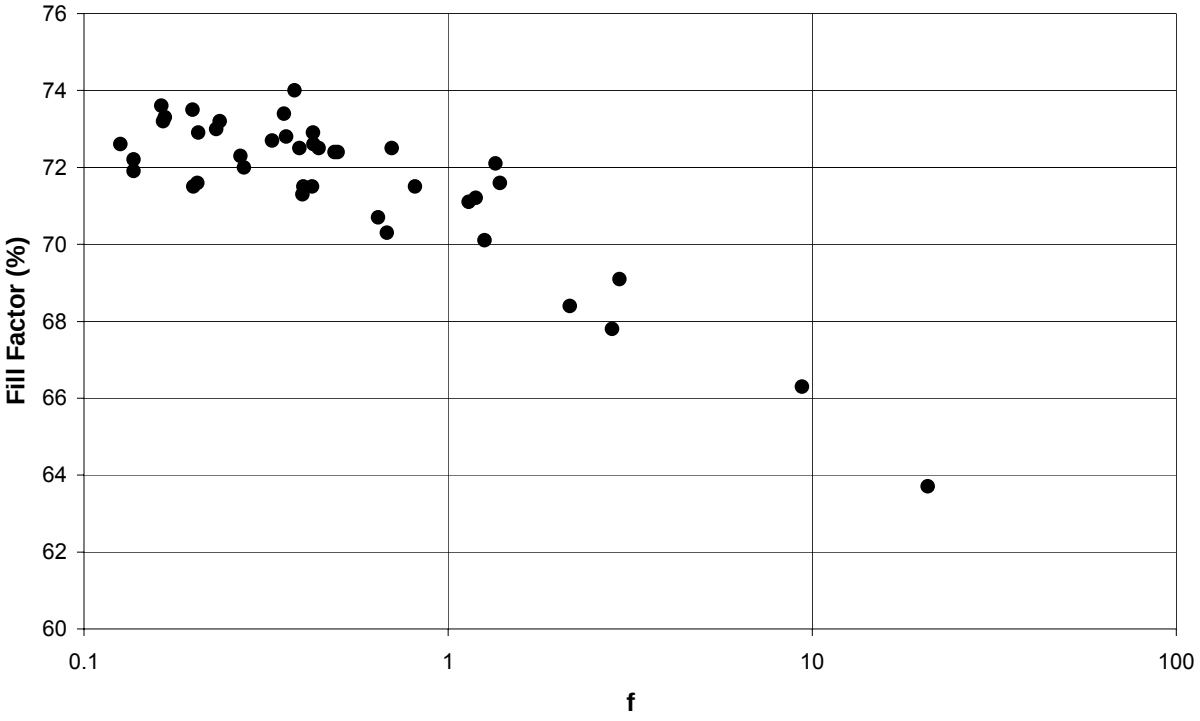

Figure 5. Dependence of fill factor on f-factor for lattice-mismatched InGaAs on InP substrates for the cells in Table 2.

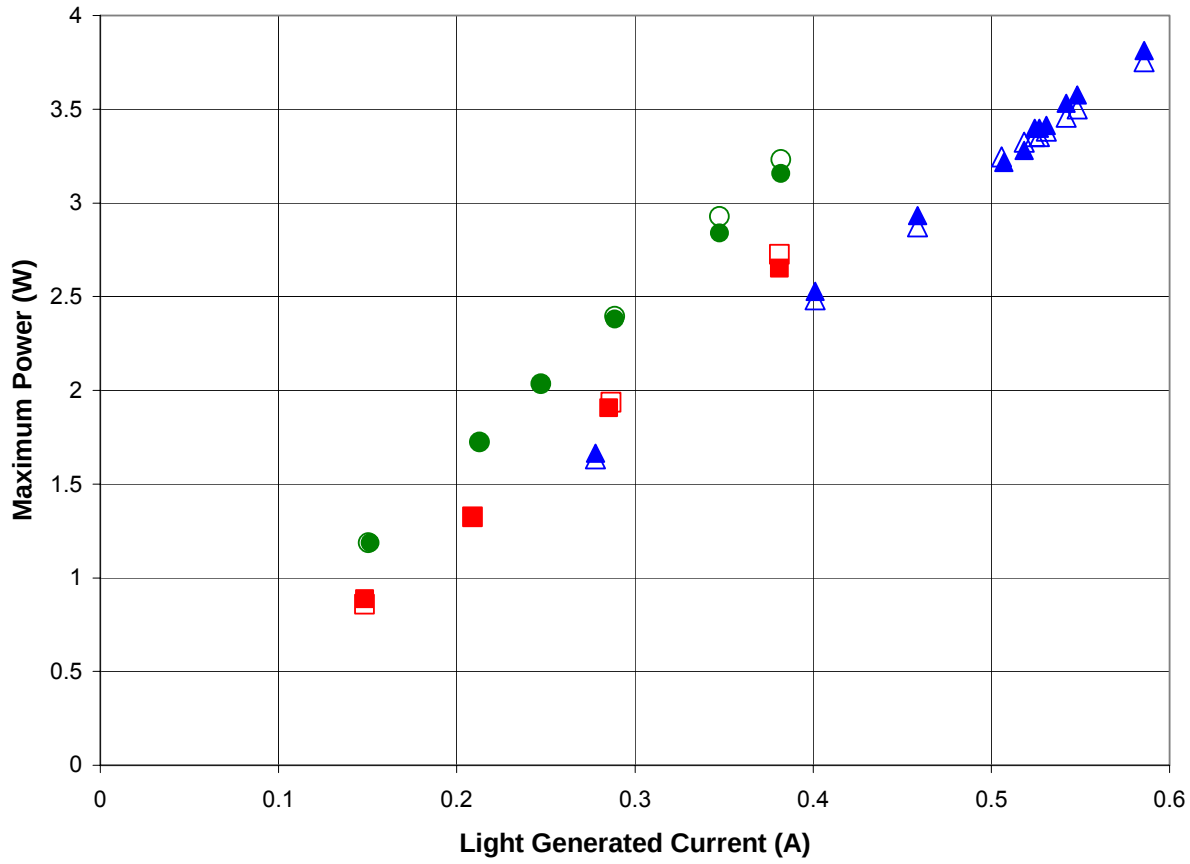

Figure 6. Graph showing good agreement between measured (solid symbols) and predicted (open symbols) power for three MIMs, using the cell parameters calculated at a single light generated current. The fits were performed at a light generated current of 0.2 - 0.25A for Samples A and B (circles and squares, respectively), and 0.45A for Sample C (triangles).

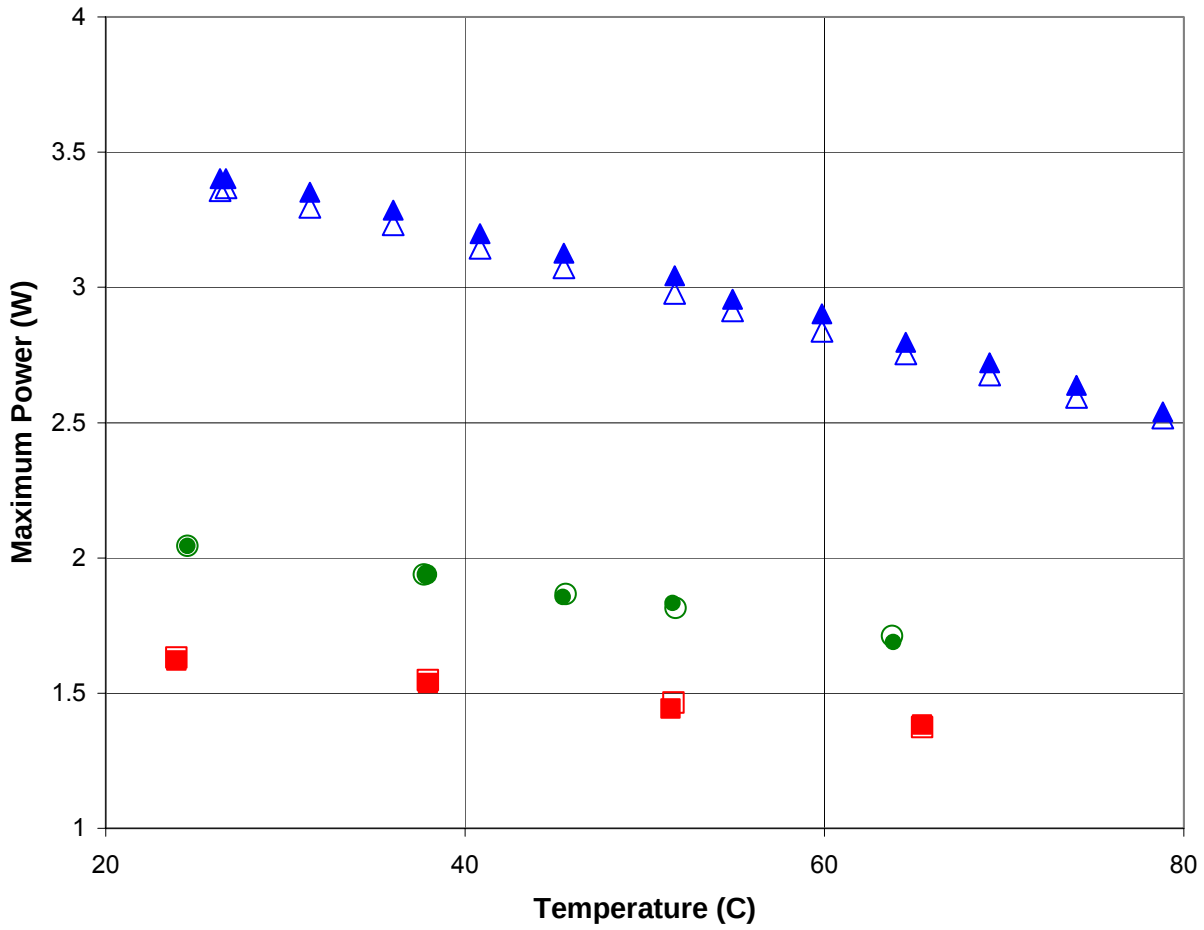

Figure 7. Graph showing good agreement between measured (solid symbols) and predicted (open symbols) power for three MIMs (Samples A, B, and C), using the cell parameters calculated at a single temperature of 25C. Data for Samples A, B, and C are represented by circles, squares, and triangles, respectively.